



The $^{24}\text{Mg}(\alpha, p)^{27}\text{Al}$ reaction measurement using solenoid spectrometer for nuclear astrophysics (SSNAP)

G. M. Gu¹ · K. Y. Chae¹ · S. M. Cha¹ · M. S. Kwag¹ · M. J. Kim¹ · J. Allen² · P. D. O'Malley² · A. Boeltzig² · A. M. Clark² · B. Frentz² · B. V. Kolk² · D. Blankstein² · D. W. Bardayan² · J. Wilkinson² · G. Seymour² · K. B. Howard² · M. Renaud² · M. R. Hall² · R. J. deBoer² · P. Huestis² · R. Kelmar² · S. Aguilar² · S. L. Henderson²

Received: 8 January 2024 / Revised: 15 March 2024 / Accepted: 18 March 2024
© The Korean Physical Society 2024

Abstract

The $^{24}\text{Mg}(\alpha, p)^{27}\text{Al}$ reaction was measured using the solenoid spectrometer for nuclear astrophysics at the University of the Notre Dame to study the astrophysical $^{24}\text{Mg}(\alpha, p)^{27}\text{Al}$ reaction rate. Alpha beams from the 10-MV FN tandem accelerator impinged on ^{24}Mg solid targets which were made using the vacuum evaporation method on ^{12}C foils. A total of 43 beam energies were used. Recoiling protons from the $^{24}\text{Mg}(\alpha, p)^{27}\text{Al}$ reaction were detected using a double-sided position sensitive silicon detector array mounted on the solenoid. Energies, times of flight, and flight distances of particles were measured for particle identification. Protons associated with a wide range of excitation energies $E_x = 12.42\text{--}14.44$ MeV in ^{28}Si were identified.

Keywords $^{24}\text{Mg}(\alpha, p)^{27}\text{Al}$ reaction · Solenoid-based spectrometer · Normal kinematics

1 Introduction

An X-ray burst can be characterized by a sudden and intense release of X-ray radiation from a compact astronomical object, typically a neutron star in a binary star system [1]. During the burst, a very large amount of energy of about $10^{36}\text{--}10^{38}$ erg/s is released. A burst typically lasts for 10–100 s, and the recurrence times range from hours to days [2]. Very high temperatures of 1–2 GK can be reached during the burst. Many proton-rich nuclei up to the Sn–Sb–Te region can be synthesized through the αp -process and the rapid proton capture process (rp -process) [3–5]. To understand the heavy-element synthesis and energy production during the burst, the knowledge of various nuclear reactions participating in the process is essential.

In the sensitivity study performed by Parikh et al. [6], the impact of uncertainties in nuclear rates on the nucleosynthesis during type-I X-ray burst was investigated. Ten different

models with characteristic temperature and density profiles were considered. It was found that the uncertainty of the $^{24}\text{Mg}(\alpha, p)^{27}\text{Al}$ reaction rate plays a crucial role in the final abundance of ^{34}S when the long burst duration model K04-B2 was used. It was also shown that the reaction rate affected the total energy output by more than 5%. Therefore, studying the $^{24}\text{Mg}(\alpha, p)^{27}\text{Al}$ reaction rate at X-ray burst temperatures is essential to better understand the X-ray burst.

Since the reaction proceeds through the ^{28}Si levels located above the α threshold at 9.984 MeV, the properties of the levels are very important for the $^{24}\text{Mg}(\alpha, p)^{27}\text{Al}$ reaction rate calculation. Although both the α particles and ^{24}Mg are stable nuclei that can be provided as the beams or targets rather easily, the results from the direct measurements of the reaction are still sparse [8, 9]. In Ref. [8], the excitation curve for the $^{24}\text{Mg}(\alpha, p)^{27}\text{Al}$ reaction was reported. By comparing the results with the excitation curves of the previously reported $^{27}\text{Al}(p, p)^{27}\text{Al}$ and $^{27}\text{Al}(p, \alpha)^{24}\text{Mg}$ experiments, the reaction Q-value was deduced. In another work by Ahn et al. [9], the secondary γ -rays from the final states in ^{27}Al ($E_x = 0.844$ and 1.014 MeV) to the ground state were measured for the $^{24}\text{Mg}(\alpha, p)^{27}\text{Al}$ reaction rates. The $^{24}\text{Mg}(\alpha, p_1)^{27}\text{Al}$ and $^{24}\text{Mg}(\alpha, p_2)^{27}\text{Al}$ channels were studied at the energy range relevant for the X-ray burst. It was found that the contribution to the total reaction rate due to the population of excited

✉ K. Y. Chae
kchae@skku.edu

¹ Department of Physics, Sungkyunkwan University, Suwon 16419, Republic of Korea

² Department of Physics and Astronomy, University of Notre Dame, Notre Dame, IN 46556, USA

states in ^{27}Al is up to 6.1% at high temperatures of above 2 GK. Although our understanding of $^{24}\text{Mg}(\alpha, p)^{27}\text{Al}$ reaction has been substantially improved through previous works, the reaction rate is still rather uncertain due to the lack of the knowledge on the resonance parameters. Therefore, further direct measurements of the $^{24}\text{Mg}(\alpha, p)^{27}\text{Al}$ reaction are needed to accurately estimate the astrophysical reaction rate.

The $^{24}\text{Mg}(\alpha, p)^{27}\text{Al}$ reaction was studied using the solenoid spectrometer for the nuclear astrophysics (SSNAP) at the University of Notre Dame (UND) [10]. The spectrometer was originally developed for the transfer reaction studies in inverse kinematics, following the principle of the helical orbit spectrometer (HELIOS) at Argonne National Laboratory (ANL) [11]. In this experiment, however, the $^{24}\text{Mg}(\alpha, p)^{27}\text{Al}$ reaction was studied using α beams and ^{24}Mg solid targets in normal kinematics to demonstrate the feasibility of using the SSNAP for compound nucleus reaction measurements. The SSNAP utilizes a 6T superconducting solenoid used for the Twinsol [12, 13] and an array of position-sensitive detectors. Type Super X3 double-sided silicon strip detectors from micron semiconductor were used for the array. Six detectors were mounted along the beam axis to measure the energies, flight distances and flight times of the particles from the reaction.

The experimental setup and procedures are detailed in Sect. 2. The preliminary results of the normalization counts obtained from the $^{24}\text{Mg}(\alpha, p)^{27}\text{Al}$ reaction measurement are described in Sect. 3. Conclusion and future plan are provided in Sect. 4.

2 Experiment

A schematic diagram of the $^{24}\text{Mg}(\alpha, p)^{27}\text{Al}$ experimental setup is shown in Fig. 1. The experiment was performed using the α beams from the 10 MV FN tandem accelerator at the Nuclear Science Laboratory (NSL). The energies of α beams ranged from 2.84 MeV to 5.20 MeV ($2.43 \text{ MeV} < E_{c.m} < 4.45 \text{ MeV}$).

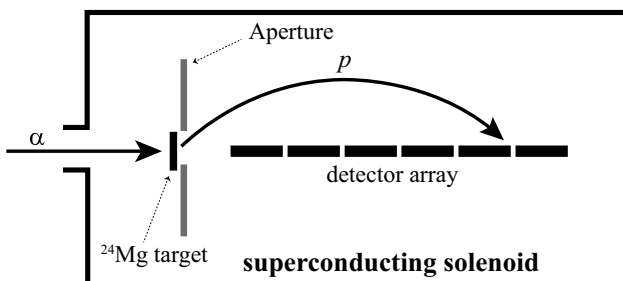


Fig. 1 A schematic diagram of the experimental setup. The protons from the $^{24}\text{Mg}(\alpha, p)^{27}\text{Al}$ reaction were detected by a detector array in the solenoid of SSNAP

$E_{c.m} < 4.45 \text{ MeV}$). The beams impinged on a $50 \mu\text{g}/\text{cm}^2$ ^{24}Mg foil target. The target was made using the vacuum evaporation method on a $5 \mu\text{g}/\text{cm}^2$ ^{12}C foil. A step size of 40 keV was taken in the bombarding energy, because the expected energy loss of the beam particles in the target is about 20–30 keV. The protons from the reaction were detected by the detector array that was installed in the solenoid. The ^{24}Mg solid targets were also placed in the solenoid with a rotatable target frame.

The detector array was composed of six double-sided position-sensitive silicon strip detectors. The front side of a detector consists of four $1.0 \text{ cm} \times 7.5 \text{ cm}$ resistive strips to measure the position of the reaction particles, while the back side of the detector has four $4.0 \text{ cm} \times 1.875 \text{ cm}$ non-resistive strips to measure the energy of the particles. The detector array was placed right above the beam axis in a straight line along the beam axis as schematically shown in Fig. 1. The energy response of each strip of detector was calibrated using an α -emitting source ^{228}Th which emits α particles with various energies (5.423, 5.686, 6.288, 6.778, and 8.784 MeV). The position response of each resistive strip was also calibrated using the source. To estimate the background events, a run with a blank target frame was also performed at each beam energy. A Faraday cup was placed downstream of the solenoid to monitor the beam current.

3 Data analysis and preliminary results

The detected light charged particles were identified using their energies, times of flight, and flight distances to the detector. The recoiling particles follow helical trajectories in the uniform magnetic field \vec{B} . The cyclotron period of a particle T_{cyc} is

$$T_{\text{cyc}} = \frac{2\pi}{B} \times \frac{m}{q_e} \text{ (s)}, \quad (1)$$

where m and q_e are the mass and charge of the particle, respectively. The period is proportional to the ratio of the mass to charge of the particle as shown in the equation. The periods of several types of charged particles are calculated and shown in Table 1.

The time of flight in this experiment was measured using the signal from the silicon detector and delayed pulse from

Table 1 The cyclotron periods in nanoseconds of several light charged particles under the uniform magnetic field of 1T, 2T, and 3T

Particles	1T	2T	3T
p	65.6	32.8	21.9
d	131.2	65.6	43.7
^3He	98.2	49.1	32.7
α	130.3	65.2	43.4

the tandem buncher. Figure 2 shows the particle identification plot obtained from the blank (left) and ^{24}Mg (right) target run. The y-axis of the figure represents the time-to-amplitude converter (TAC) signal for the time of flight, while the x-axis represents the energy of the detected particle. The plot was obtained from the $E_\alpha = 4.44$ MeV run. It is obvious from the figure that the events in the red and green contours in (b) are only observed in the ^{24}Mg target run. Considering the energies of the detected particles and the reaction kinematics, it can be concluded that the events in the red contour are the protons from the $^{24}\text{Mg}(\alpha, p_0)^{27}\text{Al}$ reaction and those in the green contour are the α particles from the $^{24}\text{Mg}(\alpha, \alpha)^{24}\text{Mg}$ reaction.

The flight distance z of a charged particle along the beam axis for the cyclotron period can be written as

$$z = v_{\parallel} T_{\text{cyc}}, \quad (2)$$

where v_{\parallel} is the laboratory velocity of the particles parallel to the beam axis as shown in Fig. 3.

Figure 4 shows the energy versus position plot for the detected particles, where the position is the flight distance z in Eq. 2. Similarly to Fig. 2, the panels (a) and (b) of the figure show the results from the blank run and ^{24}Mg target run, respectively. Since a group of events are only evident in the panel (b) at the energy of about 2.6 MeV, a cut using the TAC was made. The result is shown in the panel (c). The events falling in the red contour and the green contour were also identified as the ground state transition proton from the $^{24}\text{Mg}(\alpha, p_0)^{27}\text{Al}$ reaction and the α particles from the $^{24}\text{Mg}(\alpha, \alpha)^{24}\text{Mg}$ reaction, respectively.

The identified protons and α particles were counted and normalized with the beam current at each beam energy.

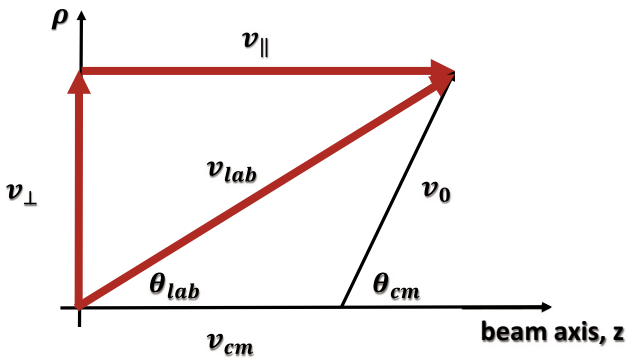


Fig. 3 The vector diagram of a particle with the velocity measured in laboratory frame v_{lab} . The vectors v_{\perp} and v_{\parallel} are the vertical and parallel components of v_{lab} , respectively. v_o is the particle velocity measured in the center of mass frame. v_{cm} is the velocity of the center of mass system. θ_{lab} and θ_{cm} are the angles of particles measured in the center of mass and laboratory frames, respectively

The incident beam energy was converted to the center of mass energy for the plot. The black and red dots in Fig. 5 indicate the normalized counts obtained from the $^{24}\text{Mg}(\alpha, p_0)^{27}\text{Al}$ reaction and the $^{24}\text{Mg}(\alpha, \alpha)^{24}\text{Mg}$ reaction, respectively. Using the α beams at the energy range of 2.84 MeV $< E_{\text{beam}} <$ 5.2 MeV (2.43 MeV $< E_{\text{c.m.}} <$ 4.46 MeV), the excitation energy in ^{28}Si from 12.42 MeV to 14.44 MeV could be investigated. For further analysis, the uncertainty in $E_{\text{c.m.}}$ will be deduced by considering the energy loss of the beam particles in the target. The resolutions in energy and position information will be thoroughly investigated as well. More precise beam current will be extracted at each beam energy. Finally, the excitation function of the reaction will be deduced.

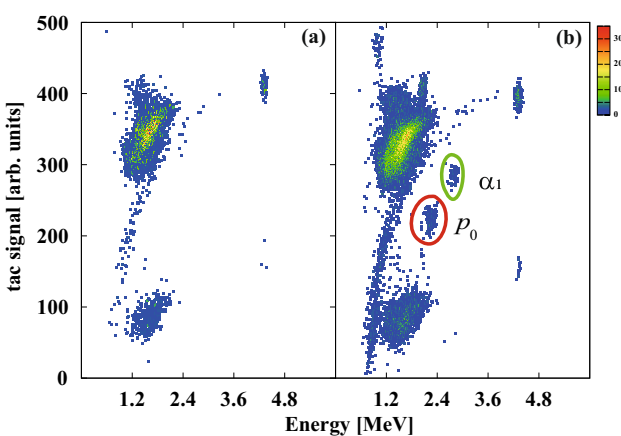


Fig. 2 A particle identification plot obtained from the (a) blank run and (b) ^{24}Mg target run. The α beam energy was 4.44 MeV in this specific case. Events within the red and green contour in (b) were identified as the protons from the $^{24}\text{Mg}(\alpha, p_0)^{27}\text{Al}$ and the α particles from the $^{24}\text{Mg}(\alpha, \alpha)^{24}\text{Mg}$ reaction, respectively

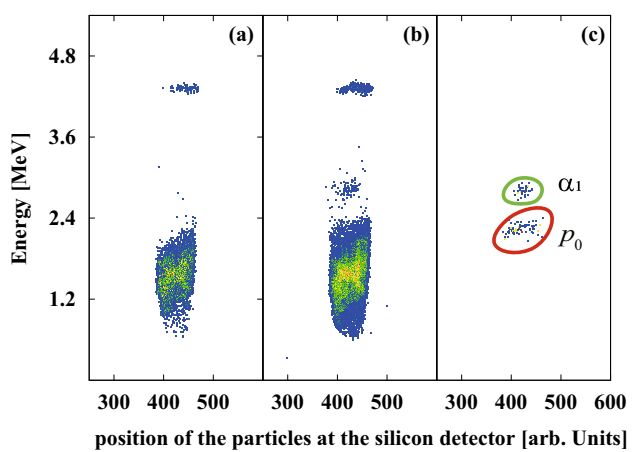


Fig. 4 The energy versus position plots for the detected particles for the (a) blank frame run and (b) ^{24}Mg target run. A cut is made using the TAC to clearly identify the p_0 and α_1 particles as shown in panel (c)

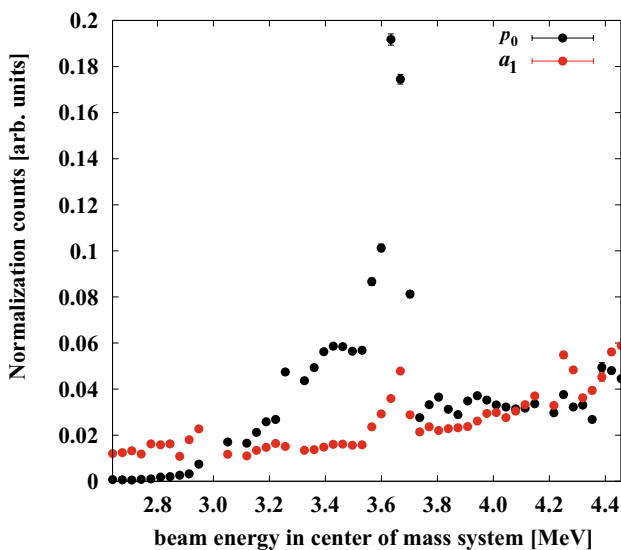


Fig. 5 A preliminary result of the normalization counts from the measurements. The black and red dots are the results obtained from the $^{24}\text{Mg}(\alpha, p_0)^{27}\text{Al}$ and $^{24}\text{Mg}(\alpha, a_1)^{24}\text{Mg}$ reaction, respectively

4 Conclusion and future plan

The $^{24}\text{Mg}(\alpha, p)^{27}\text{Al}$ reaction was measured using the solenoid spectrometer SSNAP in UND to demonstrate the feasibility of using the device for compound nucleus measurements with light charged particle beams. The beams of α particles and the solid ^{24}Mg target were used for the experiment. The recoiling protons were detected by a position-sensitive silicon detector array which was mounted inside of the solenoid. Protons associated with a wide range of excitation energies in ^{28}Si ($12.42 \text{ MeV} < E_x < 14.44 \text{ MeV}$) were identified. Events from the $^{24}\text{Mg}(\alpha, a_1)^{24}\text{Mg}$ reaction were also identified through the measurements. To determine the precise differential cross sections, we will investigate the

number of incident beam particles measured by the beam monitoring system at each beam energy, the areal density of target atoms, and the solid angle covered by silicon detector strips. By comparing the empirical excitation function and the theoretical R-matrix calculations, resonance parameters such as spin, parity, and the partial width of α and protons will be extracted. The $^{24}\text{Mg}(\alpha, p)^{27}\text{Al}$ reaction rate will be studied from the resonance parameters as well.

Acknowledgements This work was supported by the National Research Foundation of Korea (NRF) grants funded by the Korea government (Grant no. 2020R1A2C1005981). This work was also supported in part by the National Science Foundation (Grant no. NSF PHY-2011890).

References

1. J.L. Fisker, H. Schatz, F.-K. Thielemann, *Astro. Phys. J. Suppl.* **174**, 261 (2008)
2. H. Schatz, K.E. Rehm, *Nucl. Phys. A* **777**, 601 (2006)
3. R.K. Wallace, S.E. Woosley, *Astro. Phys. J. Suppl.* **45**, 389 (1981)
4. R.E. Taam, *Ann. Rev. Nucl. Part. Phys.* **35**, 1 (1985)
5. H. Schatz et al., *Phys. Rev. Lett.* **86**, 3471 (2001)
6. A. Parikh et al., *Astro. Phys. J. Suppl.* **178**, 110 (2008)
7. O. Koike et al., *Astro. Phys. J.* **603**, 242 (2004)
8. S.G. Kaufmann, E. Goldberg, L.I. Koester, F.P. Mooring, *Phys. Rev.* **88**, 673 (1952)
9. T. Ahn et al., *Phys. Rev. C* **102**, 035805 (2020)
10. J. Allen et al., *Nucl. Instrum. Methods A* **954**, 161350 (2020)
11. A.H. Wuosmaa et al., *Nucl. Instrum. Methods A* **580**, 1290 (2007)
12. M.Y. Lee et al., *AIP Conf. Proc.* **392**, 397–400 (1997)
13. F.D. Becchetti et al., *Nucl. Instrum. Methods A* **505**, 377–380 (2003)

Publisher's Note Springer Nature remains neutral with regard to jurisdictional claims in published maps and institutional affiliations.

Springer Nature or its licensor (e.g. a society or other partner) holds exclusive rights to this article under a publishing agreement with the author(s) or other rightsholder(s); author self-archiving of the accepted manuscript version of this article is solely governed by the terms of such publishing agreement and applicable law.